Eur Biophys J (2016) 45:843–852
DOI 10.1007/s00249-016-1156-8

ORIGINAL ARTICLE

EBSA
Biophysics in Europe

Electrochemical impedance spectroscopy for black lipid membranes fused with channel protein supported on solid-state nanopore

Muhammad S. Khan[1] · Noura S. Dosoky[2] · Bakhrom K. Berdiev[3] · John D. Williams[1]

Received: 18 November 2015 / Revised: 25 March 2016 / Accepted: 6 April 2016 / Published online: 1 August 2016

Abstract Black lipid membranes (BLMs) have been used for detecting single-channel activities of pore-forming peptides and ion channels. However, the short lifetimes and poor mechanical stability of suspended bilayers limit their applications in high throughput electrophysiological experiments. In this work, we present a synthetic solid-state nanopore functionalized with BLM fused with channel protein. A nanopore with diameter of ~180 nm was electrochemically fabricated in a thin silicon membrane. Folding and painting techniques were demonstrated for production of stable suspended BLMs followed by incorporation of transmembrane protein, ENaC. Membrane formation was confirmed by employing electrochemical impedance spectroscopy (EIS) in the frequency regime of 10^{-2}–10^{5} Hz. Results show that electrochemically fabricated solid state nanopore support resulted in excellent membrane stability, with >1 GΩ of up to 72 and 41 h for painting and folding techniques, respectively. After fusion of ENaC channel protein, the BLM exhibits the stability of ~5 h. We anticipate that such a solid-state nanopore with diameter in the range of 150–200 nm and thickness <1 μm could be a potential platform to enhance the throughput of ion-channel characterization using BLMs.

Keywords Solid-state nanopore · Silicon · Black lipid membranes · Transmembrane protein · ENaC · Electrochemical impedance spectroscopy · Nanobiosensor

Introduction

Ion-channel proteins are one of the major targets for drug design (Overington et al. 2006), and black lipid membrane (BLM) has been chosen as a biomimetic model for development of a hybrid electrochemical biosensor to investigate protein channel events (Khan et al. 2013). Many other groups have employed supported lipid bilayers (SLBs) to produce model systems comprised of either small/large unilamellar vesicles or Langmuir–Blodgett/Langmuir–Schaefer films (Khan et al. 2013). However, steric hindrance makes the fusion procedure of transmembrane proteins in SLBs more challenging, and proteins can easily be denatured (Khan et al. 2013). To overcome these problems, some groups have tethered lipid bilayers to the underlying substrate using linker molecules, or formed a polymer cushion between the membrane and substrate (Naumann et al. 2002; Kataoka-Hamai et al. 2010). While these strategies have proven useful for incorporating proteins into lipid bilayers for biosensing (Vockenroth et al. 2008), such lipid membranes are still only accessible from the top side, limiting their utility for studying transmembrane signaling processes. An alternative approach is to produce free-standing membranes over small apertures fabricated in a substrate in the form of a BLM, where both sides of the membrane can easily be accessed, which has also been employed for investigating lipid membranes with

Electronic supplementary material The online version of this article (doi:10.1007/s00249-016-1156-8) contains supplementary material, which is available to authorized users.

✉ Muhammad S. Khan
mskhan7@illinois.edu

[1] Electrical and Computer Engineering Department, University of Alabama in Huntsville, Huntsville, AL 35899, USA

[2] Biotechnology Science and Engineering Program, University of Alabama in Huntsville, Huntsville, AL 35899, USA

[3] Department of Biomedical Sciences, Nazarbayev University School of Medicine, Astana 010000, Kazakhstan

and without transmembrane proteins (Berdiev and Benos 2006; Montal and Mueller 1972; Nelson et al. 1980; Gutsmann et al. 2015).

Traditional free-standing BLMs are formed across micrometer-sized apertures in Teflon (Phung et al. 2011; Peterman et al. 2002), plastic septa (Mayer et al. 2003), glass cover slip (Batishchev and Indenbom 2008), and Teflon-coated silicon apertures (Wilk et al. 2004) in a thin septum that separates two aqueous chambers (*cis* and *tris*), each of which accommodates an electrode connected to an amplifier (Montal and Mueller 1972). However, the mechanical instability of BLMs limits their usage to laboratory level only. The two commonest techniques to produce aperture-suspended bilayers are the Mueller–Rudin (painting) (Mueller et al. 1962; Benz et al. 1975) and Montal–Mueller (folding) methods (Montal and Mueller 1972). Other Teflon films and polystyrene cuvettes with 10–50 μm thickness have also been introduced and apertures created using microdrilling and mechanical punching techniques. However, these techniques do not provide control over the microfabrication procedure, and the lifetime of such BLMs is even <3 h (Reimhult and Kumar 2008; Kumar et al. 2011; Bally et al. 2010). The success rate for production of BLMs using painting and folding techniques is over 95 % with average life of <6 h (Bally et al. 2010). However, special control over flow rate is required to produce a robust BLM across a Teflon aperture. Moreover, it is desirable to minimize organic solvent in membranes, though reduction of organic solvent may result in less stable BLMs (Batishchev and Indenbom 2008).

Nanofabrication tools have already enabled fabrication of apertures in the range of hundreds of nanometers, much smaller than conventional, micromachined apertures (Hirano-Iwata et al. 2010). It is well known that a smaller aperture improves the stability of suspended bilayers (Römer and Steinem 2004). By integrating lipid bilayers with an array of micro/nanopores or porous membranes (Khan et al. 2013; Mayer et al. 2003; Batishchev and Indenbom 2008; Römer and Steinem 2004; Drexler and Steinem 2003; Zagnoni et al. 2009; Weiskopf et al. 2007; Hirano-Iwata et al. 2012; Buchholz et al. 2008; Han et al. 2007; Kresák et al. 2009; Pantoja et al. 2001), the impedance and stability of BLMs have been studied with and without incorporation of protein channels. However, porous templates such as porous alumina (Römer and Steinem 2004; Drexler and Steinem 2003; Kant et al. 2014; Hirano-Iwata et al. 2010), porous silicon (Weiskopf et al. 2007; Tantawi et al. 2013a), and porous silicon nitride (Korman et al. 2013) reveal unevenly distributed pores, resulting in current leakage from uncovered pores in addition to high signal-to-noise ratio (SNR) of the system. Porous alumina membrane with total covered area of 75 μm (average pore diameter 200–350 nm) (Hirano-Iwata et al. 2010) and tapered apertures in thin Si_3N_4 membrane with diameter of 20–60 μm (Hirano-Iwata et al. 2012) were reported to be more stable systems with average life of BLMs of 30 and 45 h, respectively. Very recently, a set of tapered apertures with different shapes (beak, triangular, and cylindrical) were fabricated in SU-8 photoresist with diameter ranging from 60 to 80 μm (Kalsi et al. 2014). They produced stable BLMs using painting and folding techniques with life of 36 h (triangle-shaped aperture) and 21 h (beak-shaped aperture), respectively.

Inductively coupled plasma (ICP)-enhanced reactive-ion etching (RIE), focused ion-beam (FIB) micromachining via transmission electron microscopy (TEM), and electron-beam lithography are the expensive and time-consuming techniques required to produce either a single or an array of pores in Si_3N_4 (Kumar et al. 2011; Han et al. 2007; Korman et al. 2013; Yung-Cheng et al. 2014; Studer et al. 2009; Zhu et al. 2012; Hirano-Iwata et al. 2010; Chang et al. 2006), Al_2O_3 (Venkatesan et al. 2011), and Si (Tantawi et al. 2013a; Simon et al. 2007). To minimize the cost of nanobiosensors, we present a low-cost multistep chemical etching technique to fabricate a single nanopore with diameter of ~180 nm in a thin silicon membrane without employing any electron-beam facilities. Painting and folding methods are used to produce robust, free-standing BLMs across the single nanopore. BLMs exhibit long life of about 72 and 41 h with high impedance for painting and folding techniques, respectively. ENaC is chosen in this work to be incorporated into the nanopore-suspended BLMs. Results show that membrane with high resistance is maintained with and without fusion of Na^+ channel. Therefore, such robust nanobiosensors could be utilized for high-throughput drug screening applications.

Methods

Materials and instruments

Silicon wafer polished on both sides was purchased from Silicon Valley Microelectronics, Inc. (Santa Clara, CA, USA). Stock ampoules (25 mg) of 1,2-dipalmitoyl-*sn*-glycero-3-phosphoethanolamine (DPPE) and 1,2-dipalmitoyl-*sn*-glycero-3-phosphoserine (DPPS) were purchased from Avanti Polar Lipids Inc. (Alabaster, AL, USA) and stored at −20 °C immediately after purchase. Transmembrane protein, ENaC was reconstituted in proteoliposomes as described previously (Berdiev and Benos 2006). Molecular sieves (4 Å) and nylon filter (0.2 μm) were purchased from Sigma-Aldrich Corp. (St. Louis, MO, USA). Instruments used included a white-light interferometer (WYKO NT1100), a surface profiler (TENCOR P10), a Plasma-Therm 790 series, a scanning electron microscopy

(LEO1550), and an electrochemical impedance spectroscopy (VersaSTAT MC by Princeton Applied Research, USA).

Fabrication of nanopore

The fabrication process for production of a single solid-state nanopore has been described previously (Khan and Williams 2015). Silicon-on-insulator (SOI) <100> wafer was used as substrate with dimensions of 500/2/2.5 ± 0.5 µm. A brief summary of the fabrication process is illustrated in Fig. 1. Plasma-enhanced chemical vapor deposition (PECVD) was used to deposit a 2-µm-thick Si_3N_4 layer on both sides of the SOI wafer. An array of 1 × 1 mm^2 squares was lithographically patterned on the back side of the wafer using positive resist (SPR220). Reactive-ion etching (RIE) was then performed to etch the exposed area of Si_3N_4. The square cavity in *p*-type Si was achieved using 30 % KOH at 55 °C with total etched thickness of about 500 µm, as shown in Fig. 1a. The SiO_2 layer was removed by dipping the substrate in 5 % HF for 2 min. A thin (200 nm) layer of Si_3N_4 was sputtered on the Si (*n*-type), followed by lithographic patterning and etching of square (20 × 20 μm^2) window at the membrane center. Finally, the V-shape grooved cavity in *n*-type Si membrane was produced using 10 % KOH at 20 °C for 15 min, as shown in Fig. 1b. The Si device was sandwiched between two Teflon supports, and a blue light-emitting diode was employed on the rear side of *n*-type Si, as shown in Fig. 1c. All screws were tightened gently to avoid cracking on the mounted chip. The Pt wire was immersed in aqueous electrolyte with concentration 10:40:50 (49 % HF, 95 % ethanol, and H_2O) filled in the square cavity on the back side of the SOI wafer. Potentiostatic control was applied for electrochemical etching of the solid-state nanopore in the thin silicon membrane. Potentiostatic control with current density (*J*) of 0.47 mA/cm^2 was applied to produce a pore with diameter of 180 ± 12 nm.

Preparation of BLMs

Ampoules with lipids were opened in chloroform solution and the contents transferred into prerinsed glass vials (2.0 ml). Molecular sieves (4 Å) were added to control the internal chemistry of the lipidic solution, and each vial was covered with a Teflon side screw cap. All vials were stored at −20 °C. The final volumes used to prepare the lipidic solution in this work were 100 µl for DPPE (5.0 mg/ml) and 50 µl for DPPS (5.0 mg/ml). Lipidic solution was dried under a stream of nitrogen for 20 min and resuspended in *n*-decane to final concentration of 7.5 mg/ml. To make the surface hydrophobic, the nanopore area was treated with O_2 plasma for 1 h followed by silanization using 2 % (v/v) cyanopropyldimethylchlorosilane (CPDS) in acetonitrile for 1 h at room temperature in a nitrogen-filled glove. Although BLMs exhibit reasonable impedance in painting and folding procedures across Teflon apertures of micron size, this work reveals high impedance with better stability of free-standing BLMs across nanopore area.

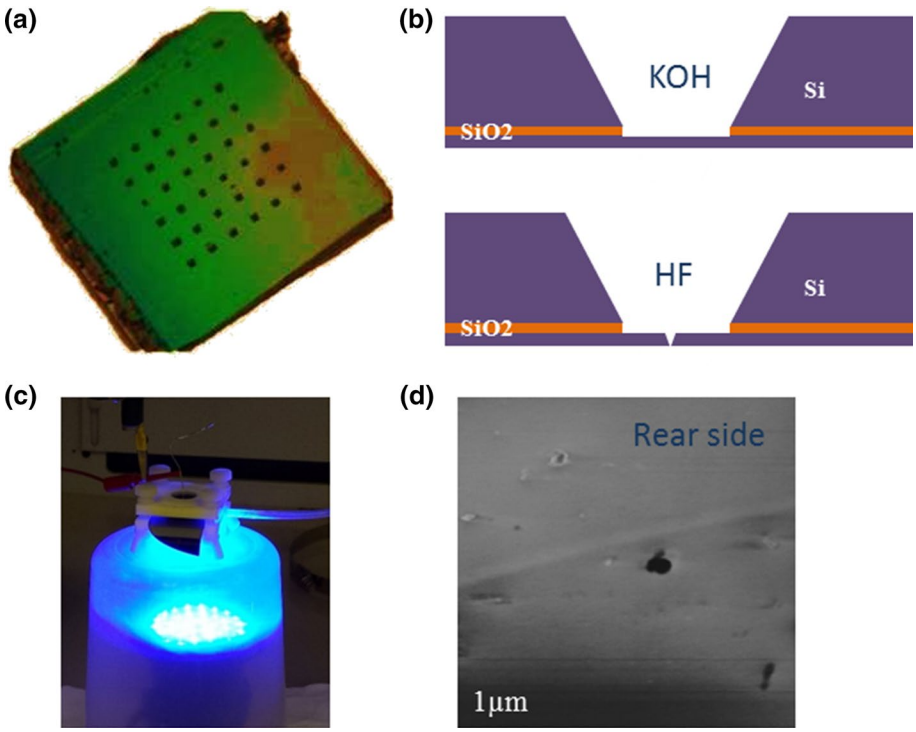

Fig. 1 Fabrication of Si-based nanobiosensor. **a** Optical image of 6 × 6 array of KOH-etched µ-cavities in Si. **b** Schematic of two-step chemical etching before and after production of single nanopore. **c** Experimental setup for electrochemical etching. **d** SEM image of electrochemically fabricated solid-state nanopore

The fabricated Si-based nanopore chip was sandwiched between two Teflon chambers (*cis* and *tris*). To optimize the rate for successful formation of BLMs and to eliminate false-positive results due to possible contaminants, both chambers were cleaned thoroughly using deionized (DI) water followed by 95 % ethanol. In the case of the folding technique, both sides of the nanopore were precoated with *n*-decane (10 µl). Filtered buffer solution (0.01 M Tris and 0.1 M NaCl) was added, and the level was set below the pore area in each chamber. Lipidic solution (100 µl) was spread on the aqueous solution near the nanopore area in each compartment. After evaporation of solvent (10–15 min), BLM was formed after gradually raising the buffer level in each compartment until it surpassed the pore opening area.

In the second method, the painting technique was used by directly applying a drop of 4 µl of lipidic solution (7.5 mg/µl) across the nanopore surface from the flat side of the thin silicon membrane using a plastic pipette tip. Excess solvent was blown away using a N_2 spray gun. A single monolayer of continuous lipid molecules was formed on the hydrophobically silanized area of the nanopore. The nanopore chip containing lipid monolayer on one side was sandwiched between two Teflon chambers. Finally, another drop (4 µl) of the same lipid composition was directly spread near the cavity area of silicon followed by filling the chambers with the same buffer.

Incorporation of ENaC into free-standing BLMs

The aim of ion-channel reconstitution is to incorporate a channel protein into an artificial membrane in which its function can be investigated. Fusion of ENaC was investigated in BLM produced using both painting and folding techniques. ENaC reconstituted in proteoliposomes (Berdiev and Benos 2006) was spread over the surface of the BLM suspended across the nanopore. Since membrane proteins are self-incorporated in BLMs, the complete fusion procedure takes about 10–15 min. Excessive disordered and unfused molecules of lipids and protein were then removed by exchanging the buffer solution. Figure 2 depicts a schematic showing the presence of free-standing BLM across the nanopore with and without incorporation of transmembrane protein.

Electrochemical Impedance Spectroscopy

The functionalized nanopore after production of BLMs with and without transmembrane protein was characterized by employing electrochemical impedance spectroscopy (EIS) in the frequency regime of 10^{-2}–10^{5} Hz. Figure 3 shows details of the experimental setup used to perform EIS. The nanopore chip was sandwiched between two

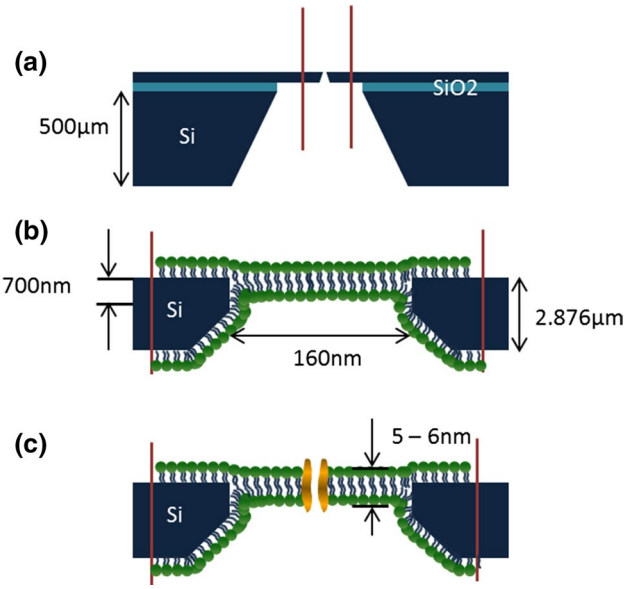

Fig. 2 Schematic of nanopore spanned by black lipid membrane with incorporated transmembrane protein. **a** Nanopore. **b** Free-standing BLM across nanopore. **c** Fused protein channel in nanopore spanned by BLM

Teflon chambers filled with buffer solution. The electrolyte (0.01 M Tris and 0.1 M NaCl) used in the Teflon chambers was filtered using 0.2-µm nylon filter. Three electrodes, comprising two Pt wires (working and counter) and one Ag/AgCl (ground), were used and immersed in the electrolyte solution. Monitoring of protein channel impedance in a membrane requires a stable and robust BLM with high resistance in the GΩ range. The thinning and stability of the BLM on the nanopore were monitored as a function of time. Electrical characterization was performed using Nyquist plots to analyze the impedance of the nanopore-spanning BLM with and without ENaC. To perform data fitting and extract information regarding the capacitance and resistance of the system, equivalent electrical models were used as described in the Electronic Supplementary Material (ESM).

There is an additional distribution of ions during the EIS experiment which reflects the nonideal behavior of the system, commonly being expressed using a constant-phase element (CPE) (Kerner and Pajkossy 1998; Kim et al. 2012). Therefore, in equivalent circuit 1 (Fig. 4a), additional parallel *RC* elements (R_{EDL} and Q_{EDL}) are introduced in series with the parallel *RC* elements of the membrane. R_{EDL} and Q_{EDL} are the charge-transfer resistance and capacitance of the electric double layer (EDL), respectively. The EDL is formed at the interface between the lipid bilayer and electrolyte. The CPE has two important parameters: α and Q. Here, Q has the same units as pure capacitance (F cm^{-2}) for $\alpha = 1$, and α is the characteristic exponent indicating

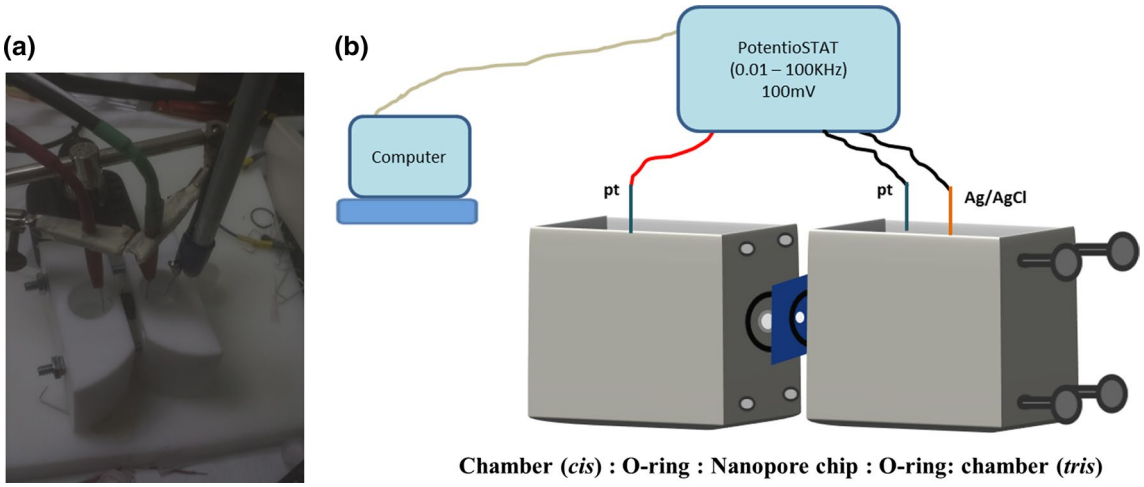

Fig. 3 Nanopore chip is sandwiched between two Teflon chambers through O-rings. Input voltage of 100 mV is applied in the frequency regime of 0.01–100 kHz using electrochemical impedance spectroscopy (EIS). Impedance spectra are monitored and recorded by computer. **a** Experimental setup showing two Teflon chambers with three electrodes. **b** Schematic of EIS setup

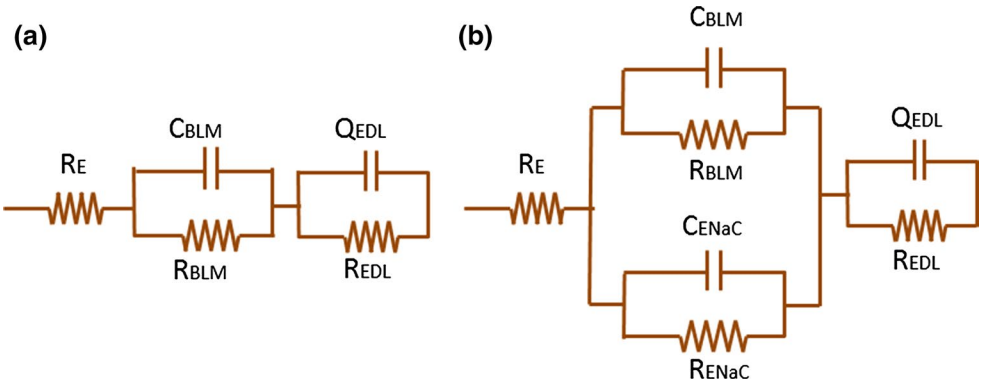

Fig. 4 Equivalent electrical models for planar bilayer lipid membrane fused with protein channel. **a** BLM suspended across nanopore chip. **b** Transmembrane protein fused in BLM across nanopore

the degree of imperfection of the CPE, varying from 0 to 1 (Macdonald and Barsoukov 2005). In the case $\alpha < 1$, Q does not represent the behavior of a capacitor; however, it is purely resistive for $\alpha = 0$. Practically α depends on the complete system behavior and helps to fit the semicircle on experimental data. Therefore, Q is commonly expressed as F $s^{\alpha-1}$ (Macdonald and Barsoukov 2005). In contrast, previously (Römer and Steinem 2004; Drexler and Steinem 2003; Wang et al. 2015), a similar membrane circuit (as described in Fig. 4) was used without considering CPE elements to study the behavior of lipid bilayers after incorporating protein channels.

Results and discussion

Any BLM used for electroanalytical experimentation must be characterized to establish the existence of the membrane and its reproducibility. The aim of this work is to obtain a membrane system attached to a solid support so that it can be applied to silicon-based chip technology with the perspective of enabling high-throughput screening assays and exhibiting high membrane impedance for the performance of single-channel measurements. Therefore, we present herein a hybrid nano-BLM system composed of black lipid membrane fused with transmembrane protein supported on a single solid-state nanopore.

Impedance spectra of BLMs

The nanopore resistance in 0.1 M NaCl electrolyte is estimated to be in the range of kΩ to MΩ (Khan and Williams 2015). After production of a free-standing BLM across the nanopore chip, the nanopore resistance increased significantly from the MΩ to GΩ range. Lipid bilayer formation was confirmed by employing electrochemical impedance spectroscopy in the frequency regime of 10^{-2}–10^{5} Hz. An impedance spectrum of nanopore-spanning BLMs for both painting and folding techniques is shown in Fig. 5. BLM formation in this study confirms the robustness and stability

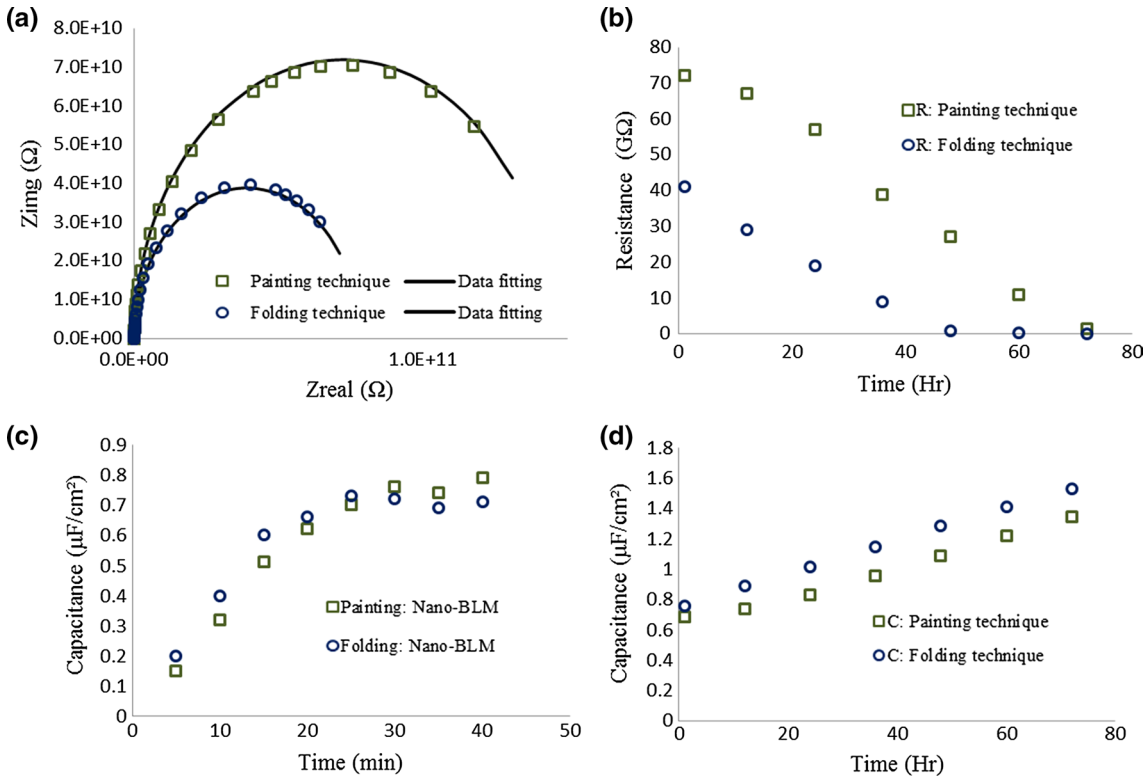

Fig. 5 Impedance spectra of nanopore-spanning BLM obtained using painting and folding techniques. **a** Nyquist plot. **b** Stability of BLMs across nanopore as function of time. **c** Thinning process and **d** capacitance of BLM suspended across single nanopore. Nanopore-spanning BLM formed using painting technique is superior to folding technique with respect to impedance (74 GΩ) and stability (72 h). BLM with painting technique (*green square*) and folding technique (*blue circle*)

of the lipid bilayer. It can be seen in Fig. 5a that membrane produced using the painting technique is more stable compared with the folding method. To obtain membrane specific parameters from the impedance spectra, the equivalent electrical models were used as illustrated in Fig. 4. The painting method exhibits high impedance of 74 GΩ, almost two times higher compared with the folding technique (41 GΩ), as shown in Fig. 5b. As long as the membrane shows resistance in the GΩ range, it is suitable for recording protein channel impedance. Solid black lines are fit curves based on the equivalent circuit, as described in Fig. 4a. The results are in good agreement with a capacitance and resistance with mean of 73.6 ± 0.21 GΩ and 0.69 ± 0.05 μF/cm^2, respectively. The mean values for a BLM produced using the folding technique for resistance and capacitance were in the order of 40.4 ± 0.37 GΩ and 0.76 ± 0.08 μF/cm^2, respectively. These values were recorded 1 h after BLM formation. Increased values in the range of 1.09 and 1.29 μF/cm^2 were observed after 48 h in case of the painting and folding method, respectively. Moreover, the electric double layer (EDL) formed at the interface of the suspended BLM and electrolyte was also included in the electrical models, resulting in R_{EDL} of 1.94 kΩ and Q_{EDL} of 9.13 μF $s^{\alpha-1}$ ($\alpha = 0.791$).

Initially, the capacitance of the BLM formed across the nanopore was not stable, and the final data were normalized after recording impedance spectra continuously for 30 min. This initial change was monitored for more than 20 free-standing BLMs prepared using the painting and folding techniques. It is estimated that the thinning process takes about 20–25 min until a stable capacitance is achieved, as shown in Fig. 5c. This could be reduced by improving the silanization and using electronic control of the buffer solution flow rate across the nanopore. Figure 5b shows the membrane resistance for BLMs as a function of time. In case of the painting method, the membrane resistance decreased from 74 to 27 GΩ in the first 48 h. On the other hand, BLM produced using the folding technique exhibited a decrease in resistance from 41 to 1.7 GΩ in the first 48 h. From statistical analysis, the lifetime of nano-BLM with membrane resistance >1 GΩ was obtained as 72 ± 4 and 50 ± 3 h for the painting and folding technique, respectively. Porous alumina membrane with total covered area of 100 μm^2 (average pore diameter 200–350 nm) was reported to be a more stable system for BLM preparation with average life of 16–30 h (Hirano-Iwata et al. 2010). However, porous alumina membrane is not biocompatible

and requires additional chemical procedures. BLMs formed from diphytanoylphosphatidylcholine (DPhPC) were more stable (up to 2–4 days) for 85–440-nm pores regularly arrayed in a silicon nitride support (Han et al. 2007). BLM life can easily be enhanced by introducing tapered aperture diameters in the range from 20 to 60 μm in thin Si_3N_4 membrane (Hirano-Iwata et al. 2010). In that work, BLMs exhibited membrane resistance higher than 1 GΩ with average life of 15–45 h. A set of tapered apertures (60–80 μm) with different shapes (beak, triangular, and cylindrical) were fabricated very recently (Kalsi et al. 2014). Kalsi et al. (2014) produced stable BLMs by using painting and folding techniques with life of 36 h (triangle-shaped aperture) and 21 h (beak-shaped aperture), respectively. One way to enhance the stability of a membrane on a single pore is to reduce the size from micrometer to nanometer range. The nanobiosensor produced in this work confirms BLM stability for ~74 h ($n = 23$) on an electrochemically fabricated single nanopore with diameter of 180 ± 12 nm in a thin silicon membrane at low cost.

It is known that the capacitance of lipid bilayers is in the range of 0.4–0.9 μF/cm^2 (Khan et al. 2013; Berdiev and Benos 2006; Montal and Mueller 1972; Römer and Steinem 2004; Cheng et al. 2001; Tantawi et al. 2013b; Ismailov et al. 1996), depending on the lipid, preparation method, and immobilization chemistry. The BLM capacitance obtained in this work is consistent with lipid bilayers produced on ordered porous silicon membrane with pore size of 7 μm (0.7 ± 0.3 μF/cm^2) (Weiskopf et al. 2007), nonordered porous silicon membrane with average pore size of ~2 μm (0.63 μF/cm^2) (Tantawi et al. 2013a; b), ordered porous alumina with pore diameter of 280 nm (0.65 ± 0.2 μF/cm^2) (Römer and Steinem 2004) and 50 nm (Drexler and Steinem 2003), and porous silicon nitride with pore size of 200 nm (0.40 μF/cm^2) (Zhu et al. 2012). The results are also in agreement with the previous team of our collaborator (Berdiev and Benos 2006). Berdiev et al. (2006) produced BLMs using the same type of lipids (DPPE/DPPS) with capacitance in the range of 0.67–0.95 μF/cm^2. The capacitance obtained in this work is also in close agreement with values obtained for closely related phospholipid phosphatidylcholine membrane in 1 mM KCl electrolyte (0.62 μF/cm^2) (Naumowicz et al. 2006a, b).

Incorporation of ENaC into BLMs

The suitability of such lipid bilayers on nanopores for development of highly sensitive biosensors was evaluated by monitoring the impedance spectra of free-standing nanopore-spanning BLMs incorporated with transmembrane protein (ENaC). BLMs with resistance >1 GΩ are required to validate the normal behavior of transmembrane protein embedded in the membrane and to record other single-ion-channel events. Reconstitution of ENaC proteins into proteoliposomes has already been discussed and published by our team (Berdiev and Benos 2006). High-transition-temperature lipids (DPPE and DPPS) are used in this work because of the ease of the fusion procedure for ENaC (Berdiev and Benos 2006; Awayda et al. 2004).

Numerous experiments were performed at different time intervals with varying concentration of ENaC (1, 2, and 3 μL) to determine the optimal concentration and long-term stability of the transmembrane protein (not discussed in this paper). Figure 6a shows the change in impedance spectra in Nyquist plots, confirming fusion of ENaC in the membrane. ENaC reconstituted in proteoliposomes (1 μl) was directly inserted in the buffer solution near the suspended BLM surface, and incorporation was then observed by noticing the dramatic decrease in membrane resistance. BLM produced with painting and folding methods showed resistance of 1.53 and 1.14 GΩ 1.5 h after fusion of ENaC in membrane, respectively. Stability of the embedded channel protein in the membrane was verified by repeating the impedance spectra continuously for 10 h in both cases. Figure 6b illustrates the behavior of membrane fused with ENaC as a function of time (h). It is noted that the impedance of BLM after inserting the Na^+ channel in both cases (painting and folding) was >1 GΩ up to 5.2 ± 0.3 h ($n = 8$). Figure 6c, d presents complete spectra in terms of magnitude and phase for nanopore-spanning BLM produced using the painting technique before and after insertion of ENaC. Figure 6c, d presents the data (experimental/simulation) for ENaC (1 μl) incorporated into BLM, recorded after 1.5 h. ENaC is functional in these experiments, as verified by comparing the trend in the impedance (GΩ) spectra with previous data (Tantawi et al. 2013a, b; Ismailov et al. 1996). Figure 6c shows that the impedance of the BLM drastically reduced to 1.53 GΩ after complete fusion of ENaC in the membrane. Figure 6d reveals the behavioral change at ~0.8 Hz in the phase spectra. The capacitance with ENaC fused in the membrane is estimated to be 0.89 ± 0.11 μF/cm^2. The result obtained in previous study by this research group using a porous silicon support was reported to be 0.54 μF/cm^2 (Tantawi et al. 2013b). This lower capacitance might be due to presence of multiple channels in the case of the nonordered porous silicon support.

Data fitting (solid black line) was performed using the electrical model as described in Fig. 4b. R_{EDL} of 1.83 kΩ and Q_{EDL} of 0.849 μF $s^{\alpha-1}$ ($\alpha = 0.752$) are the estimated values for the electric double layer (EDL) present at the interface of the electrolyte and suspended BLM with embedded ENaC. Moreover, in future experiments, authors of this work recommend using pharmacological blockers (amiloride and benzamil) to further investigate the gating characteristics (ON/OFF states) of fused ENaC in lipid bilayer suspended on solid-state nanopore.

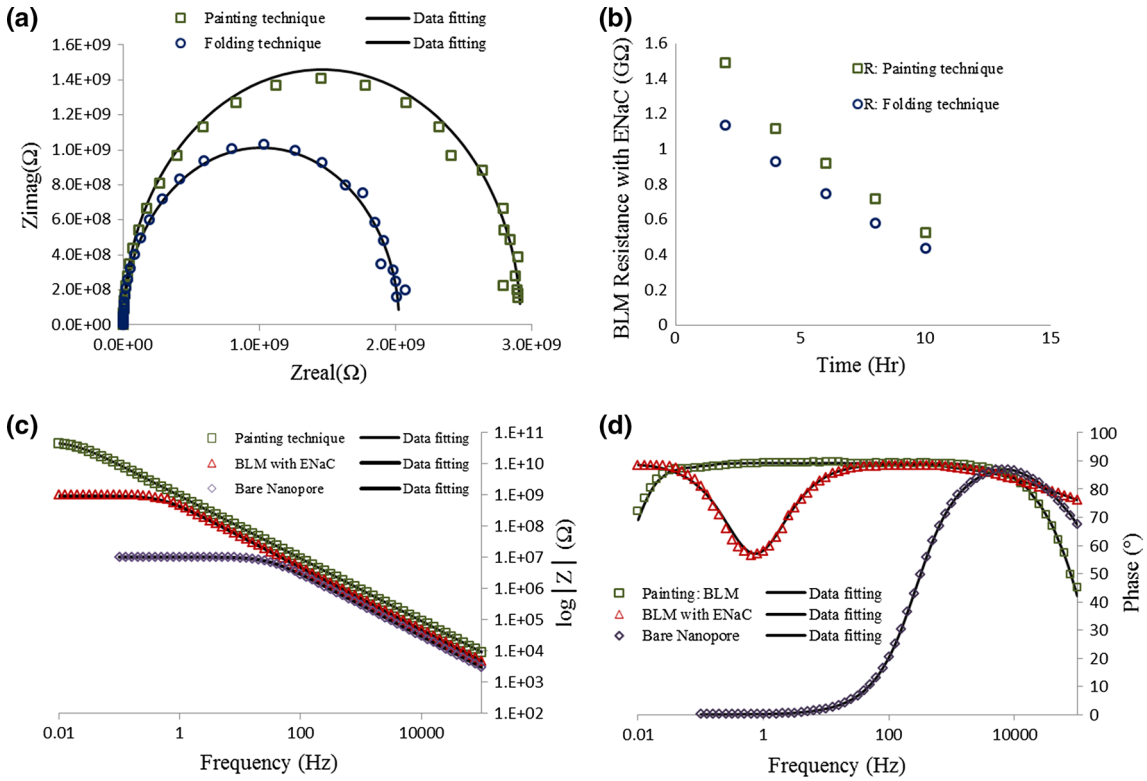

Fig. 6 Impedance spectra of BLMs (painting and folding) with embedded transmembrane protein, ENaC, supported on solid-state nanopore. **a** Nyquist plot. **b** Stability of BLMs after fusion of Na^+ channel in BLMs. **c**, **d** Bode plots. Complete impedance spectra in terms of magnitude (**c**) and phase (**d**) for nanopore-spanning BLM with painting technique before and after incorporation of ENaC. Bare nanopore (*purple diamond*), BLM with painting (*green square*), BLM with folding (*blue circle*), BLM (painting) with incorporated ENaC (*red triangle*)

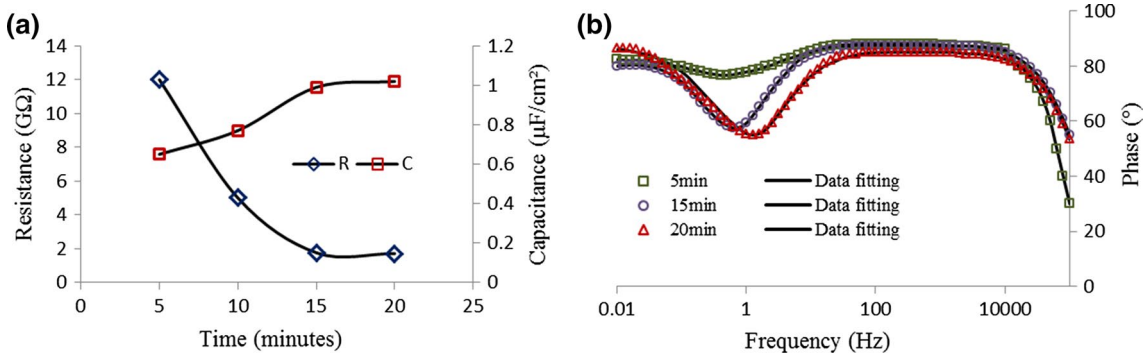

Fig. 7 Fusion of channel protein in BLM over time. **a** Time-dependent resistance and capacitance for BLM after addition of ENaC. **b** Change in BLM conductance behavior over time after addition of ENaC. BLM (painting) incorporated with ENaC (20 min, *red triangle*; 15 min, *blue circle*; 5 min, *green square*)

Time-dependent experiments for fusion of ENaC in the lipid bilayer have proven to be very sensitive. Figure 7a depicts the behavioral change of the BLM resistance and capacitance after incorporation of ENaC as a function of time. Monitoring of protein channel incorporation was carried out at different time intervals of 5, 10, 15, and 20 min. It is observed that the resistance of the system decreased with respect to time and remained constant after 15 min. Therefore, based on work carried out in this study, at least 15 min is recommended for complete fusion of the Na^+ channel in membrane composed of DPPE and DPPS. This was confirmed by noticing the dramatic decrease in membrane resistance from 12.3 to 1.75 GΩ over the time period from 5 to 15 min. A similar trend was also observed in the

case of a porous silicon support used to investigate ENaC functionality in lipid bilayers (Tantawi et al. 2013a, b). There is a minimal change in the data obtained at 15 and 20 min, confirming complete fusion of ENaC in BLM. This estimated time is in close agreement with data provided by our previous team (Berdiev and Benos 2006). However, there is a difference of 3–4 min for complete incorporation of channel protein, and this could be due to a change in the concentration of ENaC and lipids used compared with their study. A dip in Fig. 7b in the frequency range of 0.7–1.2 Hz depicts the presence of the ENaC transmembrane channel in the BLM, recording continuous flow of electrical current in terms of Na^+ ions passing through the channel protein embedded in the artificial cell membrane (BLM) supported across the solid-state nanopore biosensor.

Conclusions

This work reports the formation of defect-free BLMs on an electrochemically fabricated solid-state nanopore in a thin silicon membrane. The hybrid nanopore-based chip was composed of a functional free-standing BLM embedded with transmembrane protein. Results confirmed high impedance with good stability of the nanopore-spanning BLM. The painting technique was simple and exhibited high resistance with enhanced stability of up to 72 h as compared with the BLM produced by folding a monolayer on each side of the nanopore support. In addition, the thinning of the BLM suspended across the nanopore was investigated before running the entire impedance spectra. BLM capacitance values obtained in this study are in close agreement with results for traditional BLMs formed across Teflon apertures. ENaC incorporation in the free nanopore-spanning BLM showed good stability of up to 5 h with membrane resistance as high as 1 GΩ. This research contributes an additional step towards development of hybrid biological-solid-state nanopore for functional BLMs fused with channel protein. Such stable BLM-coated nanobiosensors have potential applications when integrated with other membrane proteins, peptides, and ion channels for drug screening applications and fourth-generation DNA sequencing.

Acknowledgments This work was supported by the Office of the Vice President for Research and Economic Development, University of Alabama in Huntsville (UAH), Huntsville, AL. Dr. Berdiev was supported, in whole or in part, by National Institutes of Health grant R21HL085112, the University of Alabama at Birmingham (UAB) Health Services Foundation General Endowment Fund, and Nazarbayev University Social Policy Grant.

Compliance with ethical standards

Conflict of interest The authors declare no conflict of interest.

References

Awayda MS, Shao W, Guo F, Zeidel M, Hill WG (2004) ENaC–membrane interactions: regulation of channel activity by membrane order. J Gen Physiol 123(6):709–727

Bally M, Bailey K, Sugihara K, Grieshaber D, Vörös J, Ständer B (2010) Liposome and lipid bilayer arrays towards biosensing applications. Small 6(22):2481–2497

Batishchev OV, Indenbom AV (2008) Alkylated glass partition allows formation of solvent-free lipid bilayer by Montal–Mueller technique. Bioelectrochemistry 74(1):22–25

Benz R, Fröhlich O, Läuger P, Montal M (1975) Electrical capacity of black lipid films and of lipid bilayers made from monolayers. Biochim Biophys Acta 394(3):323–334

Berdiev BK, Benos DJ (2006) Epithelial sodium channel in planar lipid bilayers. Methods Mol Biol 337:89–99

Buchholz K, Tinazli A, Kleefen A, Dorfner D, Pedone D, Rant U, Tampé R, Abstreiter G, Tornow M (2008) Silicon-on-insulator based nanopore cavity arrays for lipid membrane investigation. Nanotechnology 19(44):445305

Chang H, Iqbal SM, Stach EA, King AH, Zaluzec NJ, Bashir R (2006) Fabrication and characterization of solid-state nanopores using a field emission scanning electron microscope. Appl Phys Lett 88(10):103109

Cheng Y, Bushby RJ, Evans SD, Knowles PF, Miles RE, Ogier SD (2001) Single ion channel sensitivity in suspended bilayers on micromachined supports. Langmuir 17(4):1240–1242

Drexler J, Steinem C (2003) Pore-suspending lipid bilayers on porous alumina investigated by electrical impedance spectroscopy. J Phys Chem B 107:11245–11254

Gutsmann T, Heimburg T, Keyser U, Mahendran KR, Winterhalter M (2015) Protein reconstitution into freestanding planar lipid membranes for electrophysiological characterization. Nat Protoc 10(1):188–198

Han X, Studer A, Sehr H, Geissbühler I, Di Berardino M, Winkler FK, Tiefenauer LX (2007) Nanopore arrays for stable and functional free-standing lipid bilayers. Adv Mater 19(24):4466–4470

Hirano-Iwata A, Oshima A, Nasu T, Taira T, Kimura Y, Niwano M (2010a) Stable lipid bilayers based on micro- and nano-fabrication. Supramol Chem 22(7–8):406–412

Hirano-Iwata A, Taira T, Oshima A, Kimura Y, Niwano M (2010b) Improved stability of free-standing lipid bilayers based on nanoporous alumina films. Appl Phys Lett 96(21):213706

Hirano-Iwata A, Aoto K, Oshima A, Taira T, Yamaguchi RT, Kimura Y, Niwano M (2010c) Free-standing lipid bilayers in silicon chips-membrane stabilization based on microfabricated apertures with a nanometer-scale smoothness. Langmuir 26(3):1949–1952

Hirano-Iwata A, Oshima A, Mozumi H, Kimura Y, Niwano M (2012) Stable lipid bilayers based on micro- and nano-fabrication as a platform for recording ion-channel activities. Anal Sci 28(11):1049–1057

Ismailov II, Awayda MS, Berdiev BK, Bubien JK, Lucas JE, Fuller CM, Benos DJ (1996) Triple-barrel organization of ENaC, a cloned epithelial Na^+ channel. J Biol Chem 271(2):807–816

Kalsi S, Powl AM, Wallace BA, Morgan H, De Planque MRR (2014) Shaped apertures in photoresist films enhance the lifetime and mechanical stability of suspended lipid bilayers. Biophys J 106(8):1650–1659

Kant K, Kurkuri M, Yu J, Shapter JG, Priest C, Losic D (2014) Impedance spectroscopy study of nanopore arrays for biosensing applications. Sci Adv Mater 6(7):1375–1381

Kataoka-Hamai C, Higuchi M, Iwai H, Miyahara Y (2010) Detergent-mediated formation of polymer-supported phospholipid bilayers. Langmuir 26(18):14600–14605

Kerner Z, Pajkossy T (1998) Impedance of rough capacitive electrodes: the role of surface disorder. J Electroanal Chem 448(1):139–142

Khan M, Williams J (2015) Fabrication of solid state nanopore in thin silicon membrane using low cost multistep chemical etching. Materials 8(11):7389–7400

Khan MS, Dosoky NS, Williams JD (2013) Engineering lipid bilayer membranes for protein studies. Int J Mol Sci 14:21561–21597

Kim CH, Kisiel K, Jung J, Ulanski J, Tondelier D, Geffroy B, Bonnassieux Y, Horowitz G (2012) Persistent photoexcitation effect on the poly(3-hexylthiophene) film: impedance measurement and modeling. Synth Met 162(5–6):460–465

Korman CE, Megens M, Ajo-Franklin CM, Horsley DA (2013) Nanopore-spanning lipid bilayers on silicon nitride membranes that seal and selectively transport ions. Langmuir 29(14):4421–4425

Kresák S, Hianik T, Naumann RLC (2009) Giga-seal solvent-free bilayer lipid membranes: from single nanopores to nanopore arrays. Soft Matter 5(20):4021

Kumar K, Isa L, Egner A, Schmidt R, Textor M, Reimhult E (2011) Formation of nanopore-spanning lipid bilayers through liposome fusion. Langmuir 27(17):10920–10928

Macdonald JR, Barsoukov E (eds) (2005) Impedance spectroscopy: theory, experiment, and applications. Wiley, Hoboken

Mayer M, Kriebel JK, Tosteson MT, Whitesides GM (2003) Microfabricated teflon membranes for low-noise recordings of ion channels in planar lipid bilayers. Biophys J 85(4):2684–2695

Montal M, Mueller P (1972) Formation of bimolecular membranes from lipid monolayers and a study of their electrical properties. Proc Natl Acad Sci USA 69(12):3561–3566

Mueller P, Rudin DO, Tien HT, Wescott WC (1962) Reconstitution of cell membrane structure in vitro and its transformation into an excitable system. Nature 194:979–980

Naumann CA, Prucker O, Lehmann T, Rühe J, Knoll W, Frank CW (2002) The polymer-supported phospholipid bilayer: tethering as a new approach to substrate-membrane stabilization. Biomacromolecules 3(1):27–35

Naumowicz M, Petelska AD, Figaszewski ZA (2006a) Impedance analysis of a phosphatidylcholine-phosphatidylethanolamine system in bilayer lipid membranes. Electrochim Acta 51(24):5024–5028

Naumowicz M, Kotynska J, Petelska A, Figaszewski Z (2006b) Impedance analysis of phosphatidylcholine membranes modified with valinomycin. Eur Biophys J 35(3):239–246

Nelson N, Anholt R, Lindstrom J, Montal M (1980) Reconstitution of purified acetylcholine receptors with functional ion channels in planar lipid bilayers. Proc Natl Acad Sci USA 77(5):3057–3061

Overington JP, Al-Lazikani B, Hopkins AL (2006) How many drug targets are there? Nat Rev Drug Discov 5(12):993–996

Pantoja R, Sigg D, Blunck R, Bezanilla F, Heath JR (2001) Bilayer reconstitution of voltage-dependent ion channels using a microfabricated silicon chip. Biophys J 81(4):2389–2394

Peterman MC, Ziebarth JM, Braha O, Bayley H, Fishman HA, Bloom DM (2002) Ion channels and lipid bilayer membranes under high potentials using microfabricated apertures. Biomed Microdevices 4(3):231–236

Phung T, Zhang Y, Dunlop J, Dalziel J (2011) Bilayer lipid membranes supported on Teflon filters: a functional environment for ion channels. Biosens Bioelectron 26(7):3127–3135

Reimhult E, Kumar K (2008) Membrane biosensor platforms using nano- and microporous supports. Trends Biotechnol 26(2):82–89

Römer W, Steinem C (2004) Impedance analysis and single-channel recordings on nano-black lipid membranes based on porous alumina. Biophys J 86(2):955–965

Simon A, Girard-Egrot A, Sauter F, Pudda C, Picollet D'Hahan N, Blum L, Chatelain F, Fuchs A (2007) Formation and stability of a suspended biomimetic lipid bilayer on silicon submicrometer-sized pores. J Colloid Interface Sci 308(2):337–343

Studer A, Han X, Winkler FK, Tiefenauer LX (2009) Formation of individual protein channels in lipid bilayers suspended in nanopores. Colloids Surf B Biointerfaces 73(2):325–331

Tantawi KH, Berdiev B, Cerro R, Williams JD (2013a) Porous silicon membrane for investigation of transmembrane proteins. Superlattices Microstruct 58:72–80

Tantawi KH, Cerro R, Berdiev B, Martin MED, Montes FJ, Patel D, Williams JD (2013b) Investigation of transmembrane protein fused in lipid bilayer membranes supported on porous silicon. J Med Eng Technol 37(1):28–34

Venkatesan BM, Polans J, Comer J, Sridhar S, Wendell D, Aksimentiev A, Bashir R (2011) Lipid bilayer coated Al_2O_3 nanopore sensors: towards a hybrid biological solid-state nanopore. Biomed Microdevices 13(4):671–682

Vockenroth IK, Atanasova PP, Jenkins ATA, Köper I (2008) Incorporation of alpha-hemolysin in different tethered bilayer lipid membrane architectures. Langmuir 24(2):496–502

Wang XH, Ma S, Su Y, Zhang Y, Bi H (2015) High impedance droplet–solid interface lipid bilayer membranes. Anal Chem 87(4):2094–2099

Weiskopf D, Schmitt EK, Klühr MH, Dertinger SK, Steinem C (2007) Micro-BLMs on highly ordered porous silicon substrates: rupture process and lateral mobility. Langmuir 23(18):9134–9139

Wilk SJ, Goryll M, Laws GM, Goodnick SM, Thornton TJ, Saraniti M, Tang J, Eisenberg RS (2004) Teflon™-coated silicon apertures for supported lipid bilayer membranes. Appl Phys Lett 85(15):3307

Yung-Cheng W, Dau-Chung W, Tsan-Chu L (2014) Using focused electron beams to drill straight nanopores on a membrane. Int J Autom Smart Technol 4(3):157–162

Zagnoni M, Sandison ME, Morgan H (2009) Microfluidic array platform for simultaneous lipid bilayer membrane formation. Biosens Bioelectron 24(5):1235–1240

Zhu Z-W, Wang Y, Zhang X, Sun C-F, Li M-G, Yan J-W, Mao B-W (2012) Electrochemical impedance spectroscopy and atomic force microscopic studies of electrical and mechanical properties of nano-black lipid membranes and size dependence. Langmuir 28(41):14739–14746